The Response of a Spherical Tissue-Equivalent Proportional Counter to Different Ions Having Similar LET.

S. Guetersloh[a], T. Borak, [b], P. Taddei[b], C. Zeitlin[a], L. Heilbronn[a],
J. Miller[a], T. Murakami[c], Y. Iwata[c]

[a] Life Sciences Division, Lawrence Berkeley National Laboratory, Berkeley, California 94720

[b] Department of Radiological Health Sciences, Colorado State University, Fort Collins, Colorado 80523

[c] Department of Accelerator Physics and Engineering, National Institute of Radiological Sciences, 9-1 Anagawa 4-Chome, Inage-ku, Chiba 263, Japan

9 figures, 3 tables

Microdosimetry of High-Charge, High-Energy (HZE) Particles

ABSTRACT

The response of a Tissue Equivalent Proportional Counter (TEPC) to different ions having a similar linear energy transfer (LET) has been studied. Three ions, ^{14}N, ^{20}Ne, ^{28}Si, were investigated using the HIMAC accelerator at the National Institute of Radiological Sciences at Chiba, Japan. The calculated linear energy transfer (LET_∞) of all ions was 44 ± 2 keV/μm at the sensitive volume of the TEPC. A particle spectrometer was used to record the charge and position of each incident beam particle. This enabled reconstruction of the location of the track as it passed though the TEPC and insured that the particle survived without fragmentation. The spectrum of energy deposition events in the TEPC could be evaluated as a function of trajectory through the TEPC. Data indicated that there are many events from particles that did not pass through the sensitive volume. The fraction of these events increased as the energy of the particle increased due to changes in the maximum energy of delta rays. Even though the LET of the incident particles was nearly identical, the frequency averaged lineal energy, $\bar{y}_F$, as well as the dose averaged lineal energy, $\bar{y}_D$, varied with the velocity of the incident particle. However, both values were within 15% of LET in all cases.

INTRODUCTION

Proper interpretation and understanding of the spatial patterns of energy deposition from charged particles as they pass through and interact with tissue is becoming more important for accurate dosimetry in radiation protection and radiobiology. Medical facilities employ many different accelerated ions for use in tumor therapy (*1*,*2*). With the frequency and duration of manned space activities increasing, exposure to fast heavy ions from Galactic Cosmic Radiation (GCR) is also of growing concern (*3*,*4*). Though the relative number of high-Z, high-energy particles (HZE) is only about one percent of the GCR, their contribution to astronaut exposure is significant because absorbed dose scales approximately as Z^2(*3*,*4*).

Linear energy transfer (LET) is defined as the quotient of *dE* by *dl*, where *dE* is the mean energy-loss due to electronic and nuclear collisions and *dl* is the distance traveled by the particle (*5*). Considering only those energy transfers less than a specified value Δ, the *restricted* linear collision stopping power is found and is denoted LET_{Δ}. Including all possible energy transfers, *dE*/*dl* refers to the *unrestricted* collision stopping power, or LET_{∞} (*6*), which in this paper will be referred to as LET. The LET can be approximated using the Bethe-Bloch formula (*7*). This relationship can be used to select energies such that accelerated ions with different Z will have a similar *dE/dl*.

In radiation biology, differences in the relative biological effectiveness (RBE) of different ions is attributed, in part, to differences in the LET of the radiation (*8*). For radiation protection, a radiation weighting factor, w_r, has been defined to compensate for differences in RBE between different types of radiation (*9*). Multiplying the absorbed dose by the proper radiation weighting factor yields an equivalent dose that relates a risk to the specific exposure. For mixed fields and

radiations without a defined w_r, the ICRP gives a formula for calculating a radiation quality factor, Q, which is a function of the LET of the incident particle (*9*).

The energy distribution of electrons ejected from the path of the primary ion depends on the velocity of the incident particle, but not on its charge (*6*). Because particles with different charge but similar LET must have different velocities, one might expect that RBE might not be dependent on LET alone. Analytical approaches show that there are differences in the patterns of energy deposition within volumes exposed to different particles with similar LET (*10-13*). For example, an ion with a kinetic an energy of 800 MeV/nucleon can produce an electron with a maximum energy of about 2.5 MeV ($E = 2m_ec^2*\beta^2/(1-\beta^2) = 1.022*\beta^2/(1-\beta^2)$). This electron will have a csda range of 12.6 mm in tissue (*14*). For an ion at 100 MeV/nucleon, the maximum energy for a recoil electron is approximately 230 keV. This electron has a csda range of about 0.56 mm in tissue. Thus the higher energy particle will have a greater radial extension and a different pattern of energy deposition when passing through tissue.

Differences in RBE have been observed for high-energy charged particles with the same or similar LET. Protons were shown to be up to 1.6 times more efficient at cell inactivation than alpha particles at a similar LET of about 20 keV/μm (*15*). Protons were also seen to be more efficient than neon in the induction of chromosome interchanges and breaks when both ions had an associated LET of about 30 keV/μm (*16*). Plotting RBE as a function of LET for ^{3}He, ^{12}C, and ^{20}Ne it was shown that at a given LET, the RBE decreased as a function of increasing ion mass (*17*). One recent study also indicates that biological effectiveness may not be directly related to LET, but may also have an inverse relation to particle velocity (*18*). Thus the structure of the track surrounding the primary ion may be important in determining the amount of energy deposited in microscopic volumes.

When the range of many of the electrons produced by initial ionizations is larger than the volume of interest, energy loss by the primary particle is not identical with energy absorbed in this volume. Lineal energy, y, is defined as the quotient of energy imparted to the volume, ε, by the mean chord length, $\bar{l}$, assuming μ- randomness across that volume (*6*). Lineal energy is a stochastic quantity that varies with the random nature of energy deposition. It has the same dimensions as LET, keV/μm, but is not limited to the one-dimensional features of LET.

Rossi and Rosenzweig developed the first instrument to measure energy deposition in microscopic volumes of tissue, known as a tissue-equivalent proportional counter (TEPC) (*19*). The conventional TEPC[2] used today has a rigid wall made of tissue-equivalent (TE) plastic surrounding a gas filled cavity. Simulation of volumes having dimensions on the order of micrometers is accomplished by operating the TEPC at a reduced pressure. However, the density difference between the solid wall and the gas cavity can alter the pattern of energy deposition from that in a homogenous medium since the number of delta rays produced in a volume of material is directly related to the density of the material.

In a TEPC, when a charged ion passes from the high density wall into the low density gas, some electrons created in the wall near this interface enter the gas. For this reason there is an enhancement in energy deposition above that which would be expected from electrons produced in the gas alone. Forward moving electrons are often considered in track structure models for homogeneous materials. If, however, the model is reduced to describing dose as a function of radius from the track it is not possible to differentiate the contribution from electrons passing through a sharp density gradient. Large energy deposition events are also observed in a TEPC when the HZE particle happens to hit the rigid anode wire (*20,21*). Even with these anomalies present, studies measuring ^{56}Fe with energies of 200 to 1,000 MeV/nucleon indicate that the TEPC

can still measure absorbed dose and the distribution of energy deposition can be used to estimate the average quality of the incident radiation (*21*,*22*).

This study was designed to measure the response of a spherical TEPC to several accelerated charged particles having different charge and velocity, but similar LET. A particle spectrometer was used to record the charge and position of each incident particle both upstream and downstream of the TEPC. Frequency distributions of energy deposition (response functions) were recorded. These were converted into distributions of lineal energy, y. The frequency averaged lineal energy, $\bar{y}_F$, and dose averaged lineal energy, $\bar{y}_D$, were computed from these distributions. Because the position of the incident particle was recorded, the data could also be presented as distributions of energy deposition or lineal energy as a function of distance from the center of the sphere (i.e. impact parameter).

MATERIALS AND METHODS

Equipment and Experimental Arrangement

Three ions, ^{14}N, ^{20}Ne and ^{28}Si, were accelerated at the Heavy Ion Medical Accelerator (HIMAC) operated by the National Institute of Radiological Sciences (NIRS) in Chiba, Japan.(*23*) Originally designed for cancer therapy, (*17*) the facility has treated more than 1,000 patients with high energy carbon ions. The process of acceleration, extraction and beam transport insured that the selected ion was completely ionized. HIMAC is capable of accelerating a large selection of ions, from protons to xenon, with energies ranging from 100 to 800 MeV/nucleon. It is therefore possible to design experiments studying heavy ions relevant to radiation therapy and primary particles in the space radiation environment.

The accelerated ions were selected to have an LET that was equal to 44 ± 2 keV/μm at the gas cavity of the TEPC. The beam energies required to achieve this LET were 100, 230 and 800

MeV/nucleon, for ^{14}N, ^{20}Ne and ^{28}Si, respectively. A summary of the experiments is given in Table 1. For consistency, the same spherical TEPC with a sensitive volume having a diameter of 12.7 mm (one half inch) was used in all experiments and was identical to the instrument used in previous studies of ^{56}Fe (*20*,*21*). The density of the propane based tissue equivalent gas was set at 33 Torr to simulate a tissue diameter of 1μm (*24*). Over 10^6 events were recorded for each ion.

TABLE 1
Summary of Ions used in the Experiment

Primary Ion	Beam Exit Energy (MeV/nucleon)	Energy Incident upon TEPC (MeV/nucleon)	LET at the TEPC (keV/μm)	Residual Range of the Ion (cm-H_2O)	Velocity incident upon TEPC (v/c)	Max. Energy Electron Produced (keV)
Nitrogen	100	80	43	1.5	0.39	180
Neon	230	210	44	5.6	0.58	510
Silicon	800	780	46	33	0.84	2,400

The detector was calibrated using an internal ^{244}Cm alpha source (LET = 84.15 keV/μm) as well as an external PuBe neutron source, giving a total of four calibration points. From the internal source, alpha particles passed through a collimator giving trajectories through the center of the gas cavity and thus a simulated path of 1μm. A distribution of alpha particles interacting with the central anode of the TEPC gave a calibration point for energy depositions of about half that for diameter crossers since these particles were stopped in the anode and thus traveled about half the diameter of the gas cavity. For alpha particles nearing the end of their range, passing through the Bragg maximum, an alpha edge was also observed. For the external neutron source, the point of maximum energy deposition by recoil protons, the proton edge, was the fourth calibration from channel number to energy deposited. An EG&G ORTEC[3] Research Pulser was also used to

further establish linearity of the data acquisition system, ensuring that the four calibration points found by the source method could be related to energy deposition events in all other channels.

The TEPC was located between four position-sensitive lithium drifted silicon detectors (PSD) that served as a charged particle spectrometer as shown in Fig.1 (*25*,*26*). Two PSDs were mounted upstream of the TEPC, and two downstream. Energy loss as well as the transverse location within the detector were recorded and stored for each incident particle. The location of the PSD along the beam axis provided the third spatial dimension, z.

An additional silicon detector, labeled 3mm in Fig.1, was mounted between PSD3 and PSD4. This detector had a thickness of 3.0 mm and a radius of 1.0 cm and was used to increase the efficiency of triggering by ensuring that incident ions well outside the detection capability of the TEPC were not processed by the data acquisition logic.

Triggering was done both with and without the TEPC in coincidence with the 3mm detector. For each ion, over one million triggers were recorded in each mode. For each trigger, the signal from the TEPC was sent to an external EG&G ORTEC 142AH charge sensitive pre-amplifier and then split into two EG&G ORTEC shaping amplifiers. The difference in amplification was approximately a factor of four giving detailed information on the full spectrum of energy deposition events. The signals from each PSD, the 3mm detector and each shaping amplifier were sent to dedicated analog-to-digital converters (ADC).

Data Analysis

Off-line data processing began with analysis of the information recorded by each PSD. Since energy deposited in the PSD is proportional to the square of the charge of the ion, a prominent peak was observed for the ion accelerated. Fragments and noise contribute to smaller, less developed peaks and wide tails. Elimination of all but the main peak of the distribution of

energy deposited in all PSDs ensured that the incident primary ion passed through the entire spectrometer.

Cartesian coordinates were also returned by the PSDs. A calibration procedure using a carefully machined collimator was used to calibrate the spatial resolution of each PSD (*21*,*26*), which was found to be less than 0.2 mm. The particle coordinates were then determined in relation to the center of the TEPC, using PSD 2 and 3, and the impact parameter (IP) defined as the radial distance from the center of the TEPC.

The fluence of particles from the accelerated beam was not uniform. The data were separated into groups defined by a 1mm by 1mm grid across the transverse plane. Event size distributions measured by the TEPC for each grid were recorded and normalized to one incident particle. These where then combined to form a response function in lineal energy corresponding to uniform incident fluence. These were used to compute the moments, $\bar{y}_F$ and $\bar{y}_D$.

RESULTS

Models of the dose as a function of the radial distance from a heavy ion track have been described by Chatterjee(*10*) and Cucinotta(*11*). These were used to predict energy deposition in spherical volumes of tissue with uniform density as a function of the distance of the track from the center of the sphere (i.e.impact parameter). A plot of energy deposition as a function of impact parameter using the Cucinotta model is shown in Fig.2 for all three ions having an LET of 44 keV/μm. The solid line represents the approximation that energy transferred to the sphere is equal to energy absorbed. For this case, ε equals LET times the path-length through the sphere for a given impact parameter. The differences between the ideal case and the model reflect the production and escape of high-energy delta rays. The magnitude of this effect is greater for ^{28}Si

because the velocity and corresponding number of high-energy delta rays is greater than for neon and nitrogen at the same LET.

Fig.3 shows the frequency response function for a uniform fluence plotted as a function of energy deposited in the TEPC for each of the three ions. There is a prominent peak corresponding to an energy deposition of approximately 30 keV. There are also energy deposition events below 10 keV. The plots do not show data below 3 keV because that is where electronic noise overwhelms the signals. Plotting the data of Fig.3 as $\varepsilon * f(\varepsilon)$ gives the dose response. Differences observed in the frequency distribution for small energy depositions would be diminished because the dose is dominated by the large energy deposition events.

Fig.4 shows the frequency response functions plotted as cumulative distributions. Although there is a clear distinction between the response functions at small energy depositions, the median value for each varies by less than 3%.

An analysis was performed to determine whether the measured distributions were identical. No common probability function completely describes the distribution of energy deposition since the response of a TEPC is the result of many underlying processes. Non-parametric approaches were therefore used to compare the measured response functions. The Kolmogorov-Smirnov goodness-of-fit approach was used to test the cumulative distributions of the response functions against each other (*27*). The null hypothesis that the distributions were the same was rejected in a four-way comparison with a calculated *probability-value* less than 0.001^4 (α=0.05). The Kruskal-Wallis test, a non-parametric equivalent to the ANOVA procedure, was used to test equality of means (*28*). The null hypothesis that the distributions had the same mean value, however, could not be rejected. Thus, the response functions created by different ions having similar LET are different distributions, but have the same mean.

Fig.5 shows the distribution of energy deposition events for the three ions when the impact parameter is less than 0.8mm. This represents particles passing through the center of the spherical detector where the path length variation is less than 1%. The width of the curves represents the resolution of the system including energy straggling and proportional counter multiplication. These data are summarized in Table 2.

TABLE 2
Events with Impact Parameters less than 0.8 mm

Ion	Energy at the TEPC cavity (MeV/nucleon)	Median (keV)	Mean (keV)	Standard Deviation of the Distribution (keV)	FWHM/ Mean	LET times path length (keV)	Radial Dose Model (keV)	Radial Loss (Data)
Nitrogen	80	35	36	5.2	0.29	43	26	17%
Neon	210	36	37	5.6	0.28	44	25	16%
Silicon	780	36	36	5.4	0.29	46	25	22%

Differences between the mean energy deposited in the TEPC (column 4) and the LET approximation (column 7) are a combination of the escape of high energy delta rays created in the sensitive volume and the entrance of delta rays created in the material upstream of the sensitive volume. The radial dose model (column 8) underestimates energy deposition in the TEPC because it is based on homogeneous tissue. It thus accounts for delta ray escape but does not include the enhancement of forward moving electrons ejected from the high-density wall as the incident particle enters the gas cavity. The radial dose model predicts that about 40% of the LET escapes the spherical volume. The difference between the measured data and the LET approximation is about 20 % of LET (column 9). This suggests that the contribution from electrons produced in the forward wall, as seen in the data, amounts to an increase in the radial dose model of about 20% of LET. These values are similar to those observed for ^{56}Fe particle as reported by Rademacher(*20*)

and Gersey(*22*), and are in good agreement with the value of 20% reported by Nikjoo(*12*) using Monte Carlo calculations.

Fig.6 shows the mean energy deposition in the TEPC as a function of impact parameter. Events with impact parameters less than 6.35mm are from particles that pass through the sensitive volume of the spherical detector. For comparison purposes, the results of the LET approximation and radial dose model are also included for homogeneous density. The percent difference between the model (60% of LET) and the data (80% of LET), with respect to the model is 33% ((0.8-0.6)/0.6). Thus, energy deposition predicted by the radial dose model should be augmented by about 33% to compensate for the electrons ejected from the front wall of the detector for incident ions crossing the detector cavity.

The pronounced spike in energy deposition near 6.35 mm is the result of enhanced delta ray production in the high-density wall very near the gas-wall interface. This is similar to data reported by Rademacher(*20*) and Gersey(*21*) as well as to the results of model calculations by Nikjoo(*12*), The events having small energy deposition at impact parameters greater than 6.35 mm are from delta rays that enter the sensitive volume when a particle passes through the side wall. These are in effect electrons with a slowing down energy distribution that would be similar to delta rays created outside the volume of interest in homogeneous tissue. The relationship between primary ion energy and the range of these delta rays is shown by plotting the response functions on a log-log scale (Fig,7). Due to the lower energy of ^{14}N, resulting in a small residual range at the TEPC (Table 1, column 4), a fewer number of very large energy deposition events for particles at an impact parameter of 6.35 mm, as well as low energy depositions due to electrons entering the detector volume from larger impact parameters was observed.

The data from the radial dose model can be used to create a response function for homogeneous density based on a uniform fluence of incident particles by weighting the energy deposited by the number of particles that deposit that energy. This is represented as a dashed line for ^{28}Si in Fig.8. It shows the reduced energy deposition from delta rays escaping the spherical volume for particles that cross the detector cavity. There is also a very large number of events with small energy deposition (< 3 keV) corresponding to particles that pass near but not through the spherical volume. In reality a very large number of these events could occur because of the large range of the delta rays produced by the high energy ^{28}Si particle. The data were truncated at 3 keV to correspond to the lower limit of the TEPC because these events cannot be distinguished from electronic noise.

The measured response function is included in Fig.8 as a curve with open circles. As described above, energy deposition in the TEPC includes electrons created in the forward wall of the TEPC. To simulate this we have taken the data from the radial dose model and increased the energy deposition by 35% for all particles that enter the spherical volume, but do not adjust energy deposition for particles outside of the sensitive volume. These results were then convoluted with a normal distribution to simulate detector resolution with a FWHM of 30% (i.e. $\sigma^2 = \mu$). This combination of conditions is a very good representation of the measured data as shown by the solid line in Fig.8. Due to the curvature of a spherical TEPC, the increase of energy deposition from electrons generated in the wall will depend on the impact parameter of the incident particle. We have used a single value of 35% as a simple way to illustrate the magnitude of this for all impact parameters. This value is consistent with Monte Carlo models presented by Nikjoo (*12*).

The measured data were used to compute average values of lineal energy in order to determine if they may be used to obtain quality factors for radiation protection. The results are

listed in Table 3. It can be seen that even though the particles have a similar LET, the ratio of either $\bar{y}_F$ or $\bar{y}_D$ to LET decreased with energy or velocity. This is due to the variations in energy depositions from delta rays.

Table 3
Summary of Data Analysis

Ion	Calculated LET (keV/μm)	$\bar{y}_F$	$\bar{y}_D$	$\bar{y}_F$ / LET	$\bar{y}_D$ / LET
Nitrogen	43	44	47	1.02	1.09
Neon	44	42	48	0.95	1.09
Silicon	46	39	47	0.85	1.02

As seen in Fig. 3, there is an increasing number of events with small values of energy deposition that continues beyond the measurement capabilities of the detector due to electronic noise. Without this practical cut-off, the data would extend below 3 keV and this would have an influence on estimates of $\bar{y}_F$ and $\bar{y}_D$. We have investigated the effects of extrapolating the data into the noise and re-computing the mean values. This would result in a reduction of the frequency mean lineal energy of about 7.0 % for ^{14}N and ^{20}Ne, but as much as 15% for ^{28}Si. The dose mean lineal energy, on the other hand, is relatively insensitive to these events. The mean values, $\bar{y}_F$ and $\bar{y}_D$, were used to obtain estimates of quality factors using the Q(L) relationship recommended in ICRP 60(*9*). These data are summarized in Fig.9. Since the number of events recorded is very large, the uncertainty associated with estimates of the mean become very small because they are dividing by a very large number. Standard deviation of the summary statistics $\bar{y}_F$ and $\bar{y}_D$ ranged between 0.019 to 0.025. This translates into errors of 0.006 to 0.008 for estimates of the quality factors and are therefore not visible in Fig.9.

The first column shows the quality factor, Q(L), based on the exact value of LET for each particle. The second column shows the quality factor, Q(L), but substituting $\bar{y}_F$ for LET. The third column shows the quality factor, Q(L), but substituting $\bar{y}_D$ for LET. The fourth column uses the complete response function with the assumption that f(y) = f(L) and completing the integral:

$$\bar{Q} = \frac{\int Q(L = y) \cdot y \cdot f(y) dy}{\int y \cdot f(y) dy} \qquad \text{Eq 1}$$

The fifth column shows the result using Eq. 1 with the ICRU recommendation for q(y) rather that Q(L) (*29*,*30*). Ion track structure was shown to affect the accuracy of the average radiation quality determined from the measured distributions. For nitrogen and neon, all methods except the use of $\bar{y}_D$, gave values of Q within four percent of the ICRP 60 recommended method. For the much higher energy silicon, only the method that replaces LET with $\bar{y}_D$ was in agreement with the ICRP 60 value, within one percent.

DISCUSSION

The response of a spherical tissue equivalent proportional counter was measured for three ions having different energy and charge, but with a similar LET of 44±2 keV/μm. Gas pressure was adjusted to simulate a volume of tissue having a diameter of 1 μm. The measured data were compared with results of a model used to compute dose as a function of radial distance from the center of a track.

Particles that passed through the center of the detector deposited only about 80% of the energy expected from taking the product of the LET times the diameter. The decrease was attributed to high-energy delta rays escaping from the sensitive volume. The radial dose model

indicated that the energy loss due to escaping delta rays would result in only about 60% of the LET being deposited by particles passing through the center of the sphere. The difference between the data and the calculation was attributed to forward-moving electrons produced in the front wall of the detector. This forward contribution of electrons was not sufficient to compensate for the electrons escaping the sensitive volume. However, energy compensation from the wall exceeds energy loss from the gas when the impact parameter is greater than about 85% of the radius. It was shown that for a uniform fluence of particles at 800 MeV/nucleon, the measured distribution of energy deposition, $f(\varepsilon)$, could be reproduced computationally using the radial dose model if energy deposition for tracks passing through the sphere were enhanced by 35% and events that did not pass through the sphere were not enhanced at all.

The distributions of energy deposition events, $f(\varepsilon)$, were similar for all three ions but there were differences in the spectra for events with very small and large energy deposition. These were shown to be primarily from particles that did not pass through the sensitive volume of the detector. The number of events with very small energy depositions increased as the velocity of the particle increased. This was due to an increase in the energy and corresponding range of secondary electrons produced in the sidewalls of the detector.

Events with very large energy deposition where previously shown to be from particles that just graze the inside wall of the detector (i.e. having an impact parameter approximately equal to the radius of the gas cavity). This was also observed in the present data. However the frequency of these events diminished as the velocity of the incident particle decreased and they were almost nonexistent for ^{14}N with a velocity, $\beta = 0.39$. The ^{14}N particles were near the end of their range and were actually slowing down rapidly as they passed through the sidewall of the detector. In fact,

the path-length through the wall for grazing particles is approximately equal to the residual range and in this case particles do not emerge from the back side of the TEPC.

The data were transformed into lineal energy and used to obtain the frequency averaged and dose averaged lineal energy, $\bar{y}_F$ and $\bar{y}_D$ respectively. Even though the incident LET remained fairly constant, the ratio of either the frequency averaged or dose averaged lineal energy to LET decreased as the velocity of the incident particle increased. The frequency averaged lineal energy was particularly sensitive to the number of small energy deposition events. This becomes problematic because the signals corresponding to these events become indistinguishable from electronic noise. They are often eliminated from the spectrum with electronic discriminators even though they reflect the low LET portion of the HZE track.

The data were used to estimate quality factors for applications in radiation protection. All of the methods using the data from this TEPC produced results that were within 20% of the value of the quality factor based on the true value of LET and Q(L) from ICRP 60. Mean quality factors using $Q(L = \bar{y}_D)$ seemed to be the most stable since this quantity is not strongly influenced by changes in the number of very small energy deposition events recorded by the TEPC.

ACKNOWLEDGEMENTS

This research was supported in part by the National Institute of Health (NIH), National Cancer Institute (NCI) Training Grant 5 T3 CA09236, and in part by the National Aeronautics and Space Administration (NASA) Specialized Center of Research and Training in Radiation Health (NASA contract no. 6450938) awarded jointly to Colorado State University and Lawrence Berkeley National Laboratory (LBNL). A portion of this study was funded by the Japanese Society for the Promotion of Science (JSPS). The work of the LBNL group was supported by the NASA Space Radiation Health Program under NASA grant L14230C through the U.S.

Department of Energy under contract no. DE-AC03076SF00098. We wish to thank the staff of the Heavy Ion Medical Accelerator (HIMAC) at the National Institute of Radiological Sciences (NIRS) in Chiba, Japan for providing valuable beam time and support.

REFERENCES

1. F. Verhaegen, H. Palmans, Microdosimetric Characterization of Clinical Proton Beams, *Microdosimetry, an Interdisciplinary approach*, Edited by: D.T. Goodhead, P. O'Neill and H.G. Menzel (Royal Society of Chemistry, Cambridge, UK), (1997).
2. G. Kraft, W. Becher, K. Blasche, D. Bohne, B. Fischer, G. Gademann, H. Geissel, Th. Haberer, J. Klabunde, W. Draft-Weyrather, Th. Schwab, The Heavy Ion Therapy Project at GSI, Int. J. Radiat. Appl. Instrum., D, **19**,911-914 (1991).
3. NCRP, *Guidance on Radiation Received in Space Activities*, Report 98, National Council on Radiation Protection and Measurements, Bethesda, MD, 1989.
4. NCRP, *Radiation Protection Guidance for Activities in Low-Earth-Orbit*, Report 132, National Council on Radiation Protection and Measurements, Bethesda, MD, 2000.
5. ICRU, *Linear Energy Transfer*, Report 16, International Commission on Radiation Units and Measurements, Bethesda, MD, 1970.
6. ICRU, *Microdosimetry*, Report 36, International Commission on Radiation Units and Measurements, Bethesda, MD, 1983
7. F.H. Attix, *Introduction to Radiological Physics and Radiaion Dosimetry*, John Wiley & Sons, New York (1986).
8. NCRP, *The Relative Biological Effectiveness of Radiations of Different Quality*, Report 104, National Council on Radiation Protection and Measurements, Bethesda, MD, 1990.
9. ICRP, *Recommendations of the International Commission of Radiation Protection*, Report 60, International Commission on Radiological Protection, *Annals of the ICRP*, 21, Permagon Press, NY, 1991.

10. A. Chatterjee, H.J. Schaefer, Microdosimetric Structure of Heavy Ion Tracks in Tissue, *Rad. and Environm. Biophys.*, **13**, 215-227 (1976).

11. F.A. Cucinotta, R. Katz, J.W. Wilosn, R.R. Dubey, Heavy Ion Track-Structure calculations for Radial dose in Arbitrary Materials, NASA Technical Paper 3497 (1995).

12. H. Nikjoo, I.K. Khvostunov, F.A. Cucinotta, The Response of Tissue-Equivalent Proportional Counters to Heavy Ions, *Rad. Res.*, **157**, 435-445 (2002).

13. G. Kraft, Radiobiological Effects of Very Heavy Ions: Inactivation, Induction of Chromosome Abberations and Strand Breaks, *Nuclear Science Applications*, **3**, 1-28 (1987).

14. ICRU, *Stopping Powers for Electrons and Positrons*, International Commission on Radiation Units and Measurements, Report 37, Bethesda, MD, 1984.

15. D.T. Goodhead, M. Belli, A.J. Mill, D.A. Bance, L.A. Allen, S.C. Hall, F. Ianzini, G. Simone, D.L. Stevens, A. Stretch, M.A. Tabocchini and R.A. Wilkinson, Direct Comparison Between Protons and Alpha Particles at the Same LET, I., Irradiation Methods and Inactivation of Synchronous V79, HeLa and C3H10T1/2 Cells, *Int. J. Radiat. Biol.*, **61**, 611-624 (1992).

16. M. Durante, L. Cella, Y. Furusawa, K. George, G. Gialanella, G. Gross, M. Pugliese, M. Saito, T.C. Yang, The Effect of Track Structure on the Induction of Chromosomal Aberrations in Murine Cells, *Int. J. Radiat. Biol.*, **73**/3. 253-262 (1998).

17. Y. Furusawa, K. Fukutsu, M. Aoki, H. Itsukaichi, K. Eguchi-Kasai, H. Ohara, F. Yatagai, T. Kanai, K. Ando, Inactivation of Aerobic and Hypoxic Cells from Three Different Cell Lines by Accelerated ^{3}He-, ^{12}C-, and ^{20}Ne-ion Beams, *Rad. Res.*, **154**, 485-496 (2000).

18. E.H. Goodwin, S.M. Bailey, D.J. Chen, M.N. Cornforth, The Effect of Track Structure on Cell Inactivation and Chromosome Damage at a Constant LET of 120 keV/μm, Advances in Space Research, **18**, 93-98 (1996).

19. H.H. Rossi, W. Rosenzweig, A Device for the Measurement of Dose as a Function of Specific Ionization, *Radiology*, **64**, 404-411 (1955).

20. S. Rademacher, T. B. Borak, C. Zeitlin, L. Heilbronn, J. Miller, Wall Effects Observed in Tissue-Equivalent Proportional counters from 1.05 GeV/nucleon Iron-56 Particles. *Rad. Res*. **149**, 387-395 (1998).

21. B. B. Gersey, T. B. Borak, S. B. Guetersloh, C. Zeitlin, J. Miller, L. Heilbronn, T. Murakami, Y. Iwata, The Response of a Spherical Tissue-Equivalent Proportional Counter to ^{56}Fe Particles from 200-1000 MeV/nucleon., *Rad. Res.* **157**, 350-360, (2002).

22. A.S. Johnson, G.D. Badhwar, M.H. Golighty, A.C. Hardy, A. Konradi and T. Yang, *Spaceflight Radiation Health Program at the Lyndon B. Johnson Space Center*, NASA Technical Memorandum 104782, 1993.

23. Y. Hirao, H. Ogawa, S. Yamada, Y. Sato, T. Yamada, K. Sato, A. Itano, M. Kanazawa, K. Noda and S. Matsumoto, Heavy ion synchrotron for medical use HIMAC project at NIRS-JAPAN, *Nucl. Phys. A*. **538**, 542–550 (1992).

24. A.J. Waker, Principles of Experimental Microdosimetry, Rad.Prot.Dos., Vol. 61, no.4, pp. 297-308 (1995).

25. C.J. Zeitlin, K.A. Frankel, W. Gong, L. Heilbronn, E.J. Lampo, R. Leries, J. Miller and W. Schimmerling, A Modular Solid State Detector for Measuring High energy Heavy Ion Fragmentation near the Beam Axis, Rad. Meas. **23**(1), 65-81 (1994).

26. M. Wong, W. Schimmerling, W.M. Phillips, B.A. Ludewigt, D.A. Landis, J.T. Walton and S.B. Curtis, The multiple Coulomb scattering of very heavy charged particles, *Med. Phys*. **17**, 163-171 (1990).

27. W.J. Conover, *Practical Nonparametric Statistics*, John Wiley & Sons, New York, (1971).

28. R.J. Larsen, M.L. Marx, *An Introduction to Mathematical Statistics and Its Applications*, 2d. Ed., Prentice-Hall, New Jersey, (1986).

29. ICRU, *The Quality Factor in Radiation Protection*, Report 40, International Commission on Radiation Units and Measurements, Bethesda, MD, 1986.

30. A.M. Kellerer, K. Hahn, The Quality Factor for Neutrons in Radiation Protection: Physical Parameters, *Radiat. Prot. Dos.*, **23**, 1/4, 73-78 (1988).

FOOTNOTES

1. Author to whom correspondence should be addressed at Department of Radiological Health Sciences, Colorado State University, Fort Collins Co 80523, e-mail: thomas.borak@colostate.edu.
2. Far-West Technologies, Inc., 330 South Kellogg Ave., Goleta, CA 93117.
3. EG&G ORTEC, 100 Midland Rd., Oak Ridge, TN 37830.
4. The data analysis for this paper was generated using SAS software. Copyright, SAS Institute Inc. SAS and all other SAS Institute Inc. product or service names are registered trademarks or trademarks of SAS Institute Inc., Cary, NC, USA

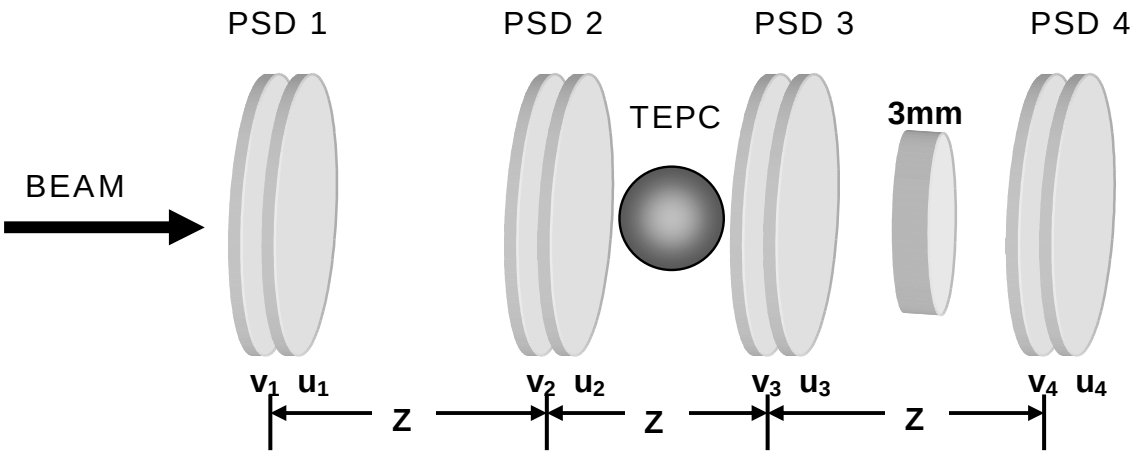

Fig.1. Schematic diagram of the experimental method. Position sensitive silicon detectors measured the horizontal and vertical coordinates of each incident particle (u,v). The distance between PSD groups, Z_{ij}, represented the third coordinate used to re-create the particle trajectory.

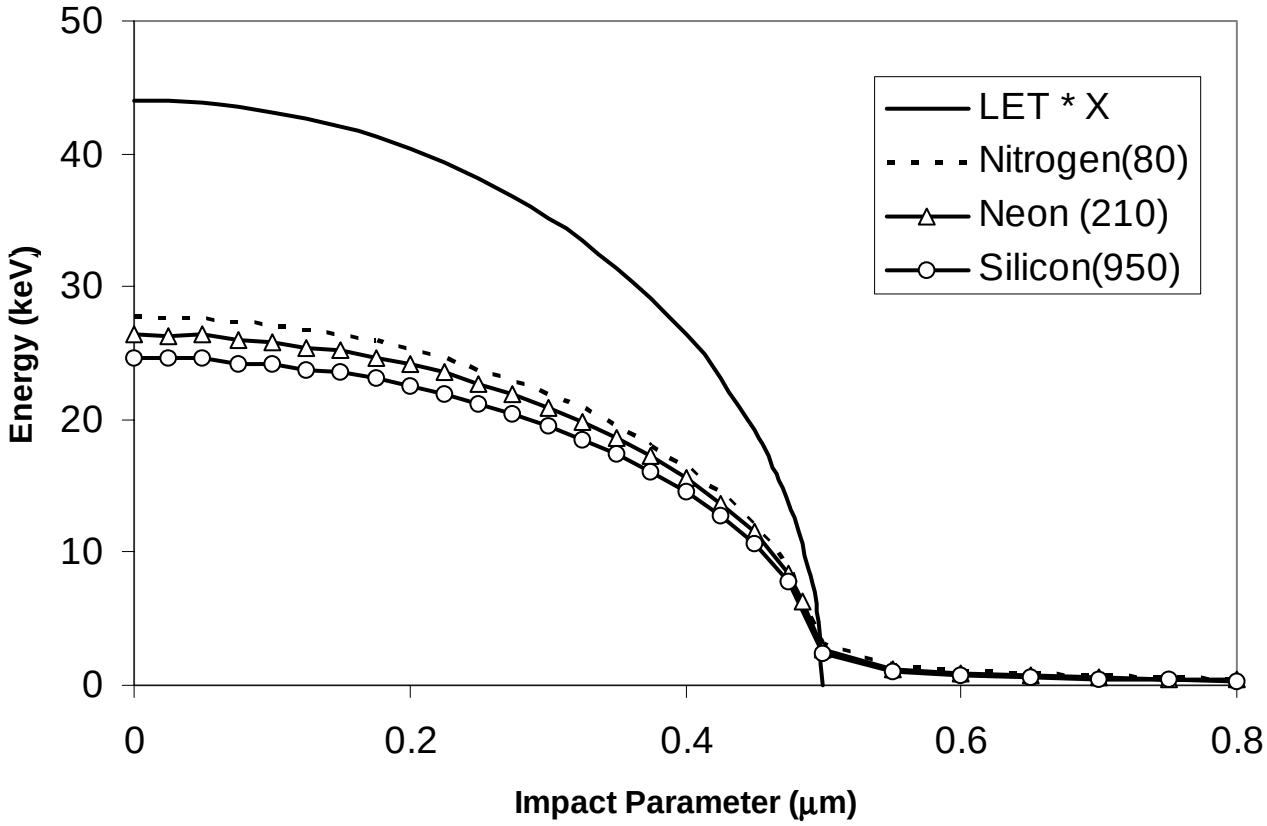

Fig.2. Energy deposition in the TEPC as a function of impact parameter. The ideal energy deposition considered to be LET times the path length through the sensitive volume for each impact parameter is shown as a solid line. Computations of energy deposition for particles having an exact LET of 44 keV/μm using the radial dose model are shown for ^{14}N (---), ^{20}Ne (-Δ-) and ^{28}Si (-o-). In this calculation, Si required a greater energy per nucleon than was measured.

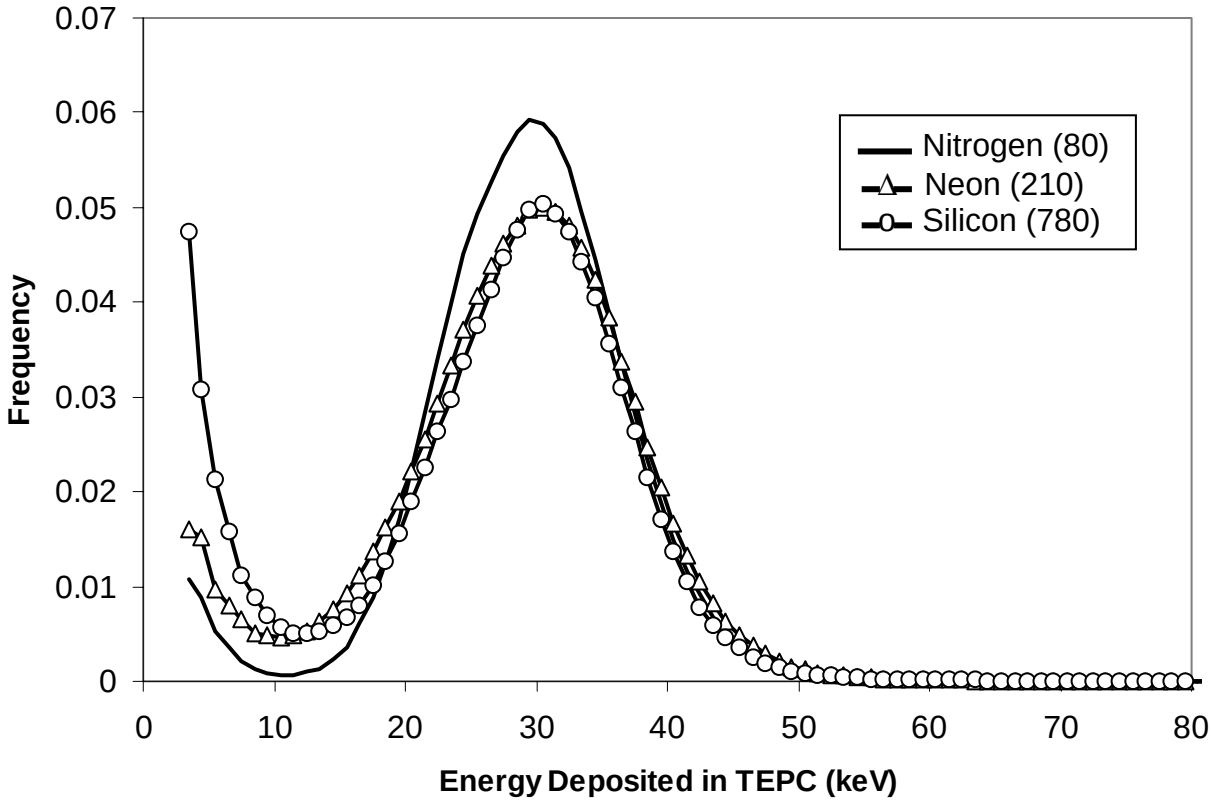

Fig.3. Frequency distributions (response functions) of energy deposition measured in the TEPC for a uniform fluence of three ions having similar LET. Each distribution has been normalized to unity. The energy of the incident ion is shown in parentheses within the insert.

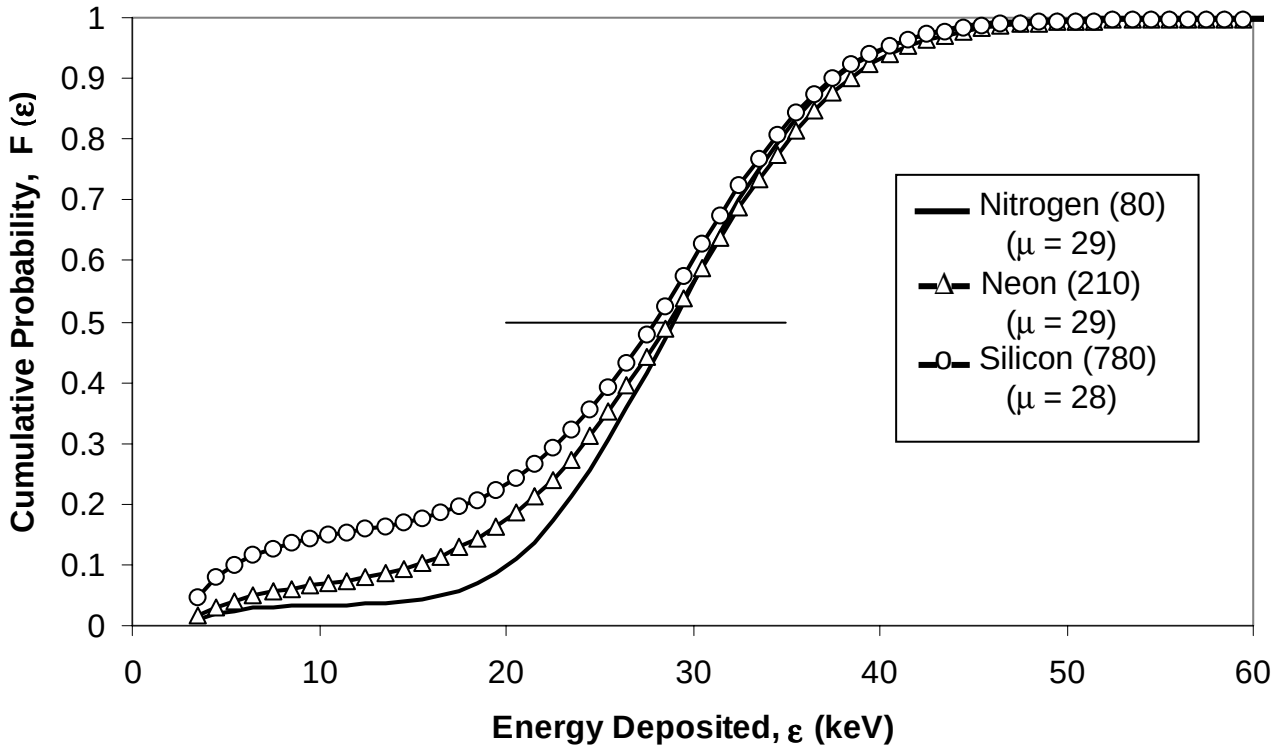

Fig.4. Cumulative distributions for the response functions measured with the TEPC for three ions having similar LET.. The horizontal line represents corresponds to 50% cumulative probability. The energy deposition in keV for this probability is shown by the numbers in parenthesis within the insert.

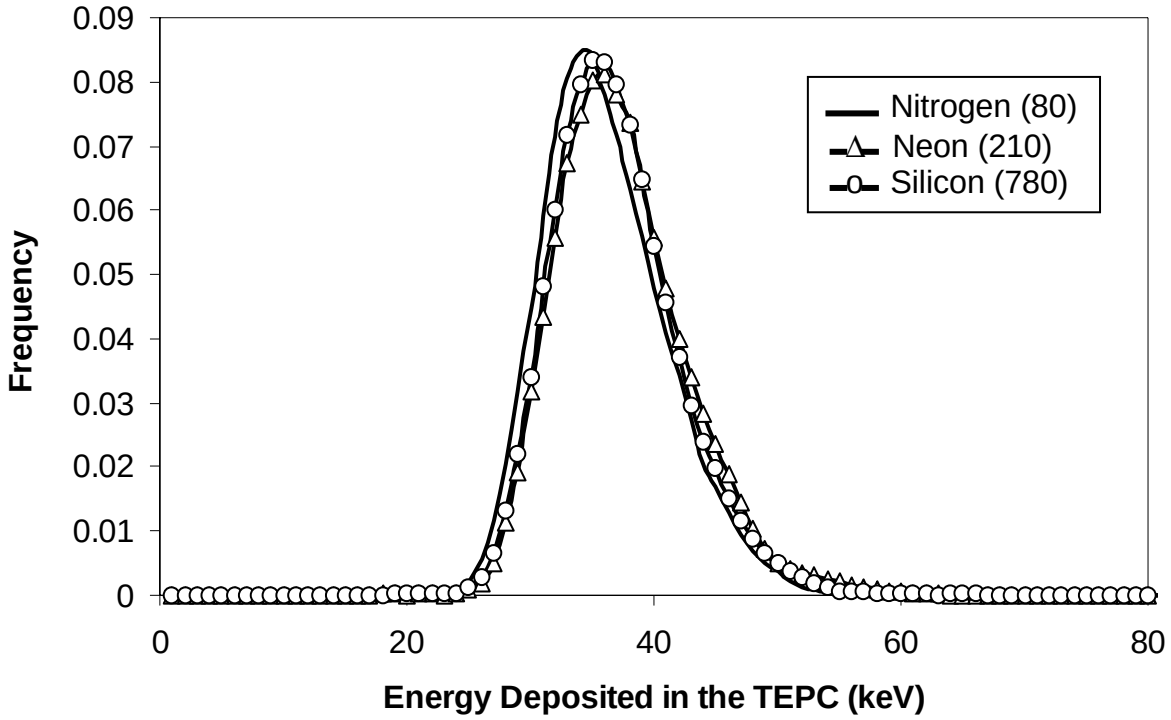

Fig.5. Energy Deposition for particles having impact parameters less than 0.8 mm. All distributions have a FWHM of about 30 %. Because path lengths through the TEPC vary by less than 1.0% for this range of impact parameters, the width of the distributions is therefore representative of the detector and system resolution.

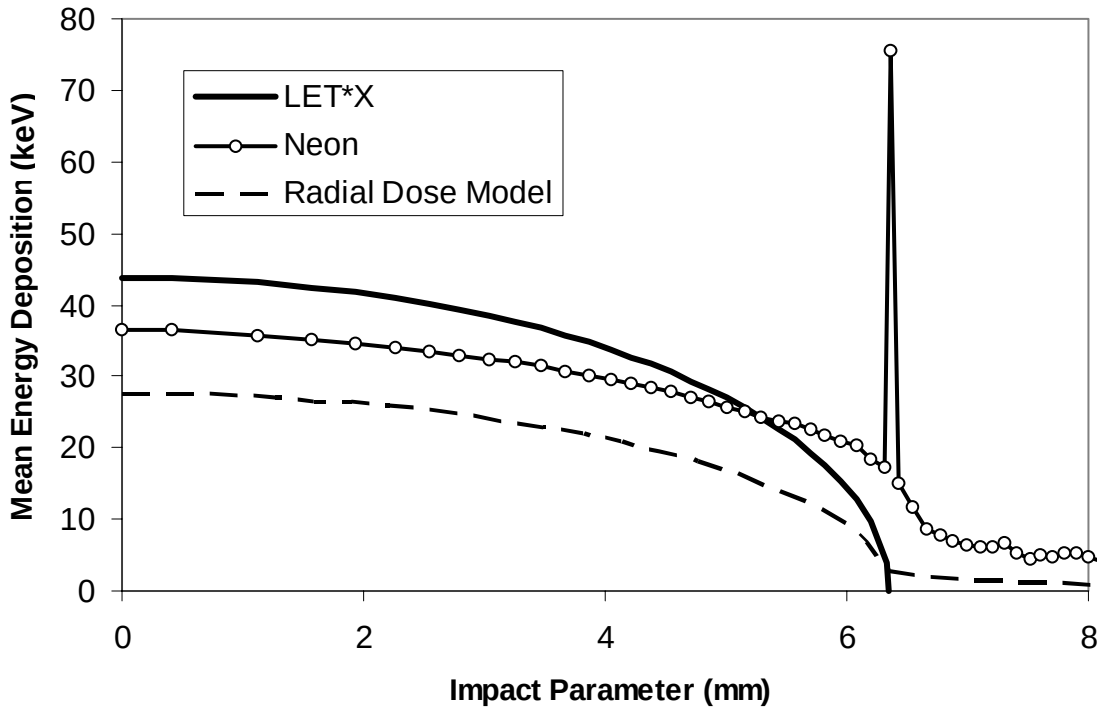

Fig.6. Mean energy deposited by ^{20}Ne at 210 MeV/nucleon as a function of impact parameter. Circles represent measured data. Smooth thick line represents the approximation of LET times path length. Dashed line shows results of the radial dose model assuming a homogenous medium.

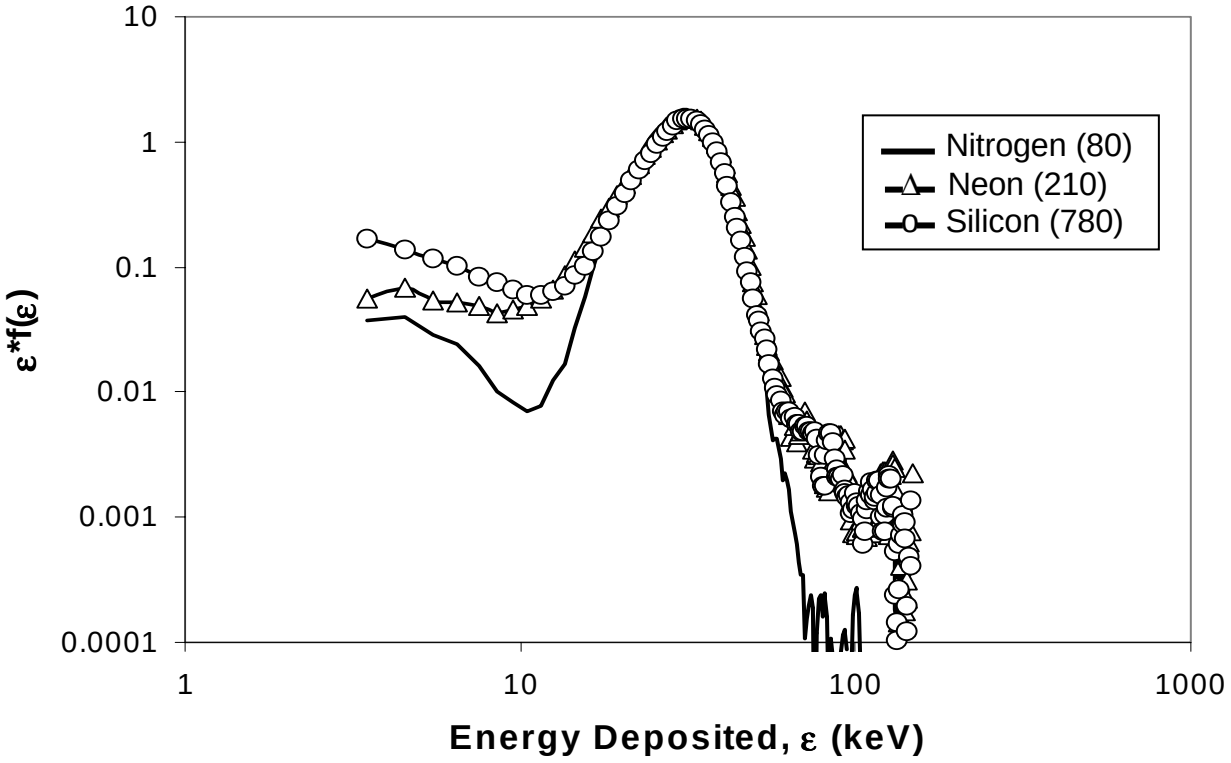

Fig.7. Measured response functions for the TEPC plotted on a log-log Scale. Energy depositions above about 60 keV are from particles with impact parameters equal to the cavity radius. Energy depositions below about 10-12 keV are due to particles passing just outside the detector cavity, entirely through the TEPC wall. These energy depositions do not occur for the ^{14}N data because the particle is slowing down and stopping in the side wall of the TEPC.

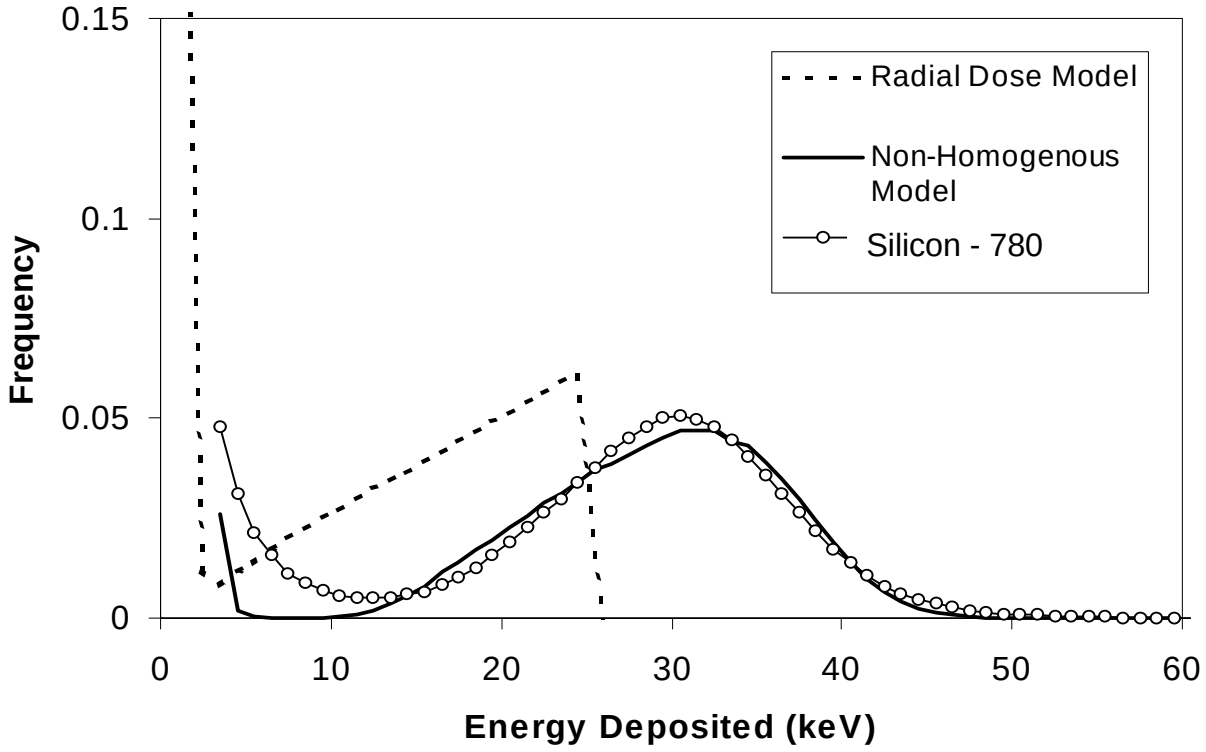

Fig.8. Comparison of energy deposition in a spherical volume for ^{28}Si at 780 MeV/nucleon. The dashed line (---) shows a computation using the radial dose model for homogeneous medium. The solid line (—) shows the results with energy deposition enhanced by 35% for particle passing through the sphere, and then convoluted with a normal distribution (FWHM = 30%) to simulate detector resolution. Measured data with the spherical TEPC is shown by circles (-o-).

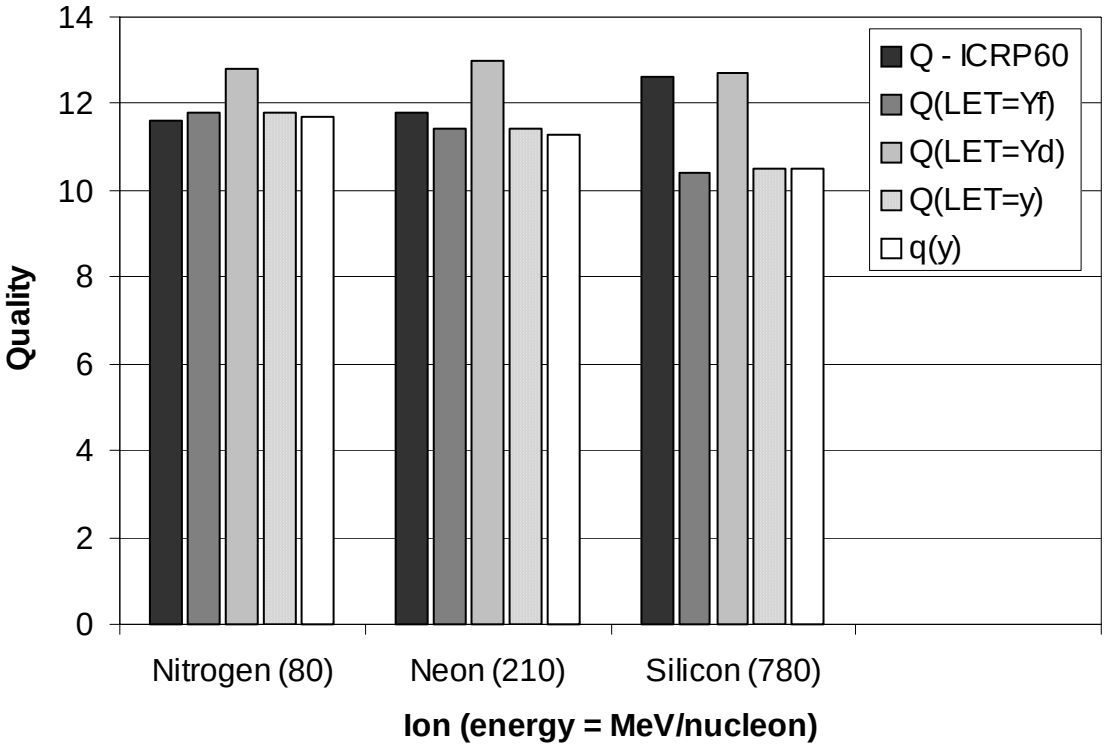

Fig.9. Computations of Quality Factors from TEPC measurements based on LET, $\bar{y}_F$, $\bar{y}_D$ and lineal energy, y. The energy of the incident ion, in MeV/nucleon, is shown in parenthesis along the abscissa.